ORIGINAL PAPER

Enhanced electrical conductivity and mechanical property of SBS/graphene nanocomposite

Hui Li · Siduo Wu · Jinrong Wu · Guangsu Huang

Abstract Styrene-butadiene-styrene tri-block copolymer/ graphene (SBS/GE) nanocomposites were prepared by solution mixing and in situ reduction of graphene oxide using hydrazine hydrate. The dispersion state of graphene was examined by XRD and optical examination, which indicates that the graphene nanosheets are well exfoliated and dispersed in the SBS matrix. The interfacial interaction between graphene and SBS was investigated by sedimentation experiment in toluene. After dissolving of the SBS/GE nanocomposite, the graphene nanosheets do not separate from the solution, moreover, even after prolonged ultracentrifugation, a dark-colored supernatant with graphene suspension is still retained, suggesting that the graphene nanosheets are stabilized in the solution with the attached SBS molecules due to the existence of strong interfacial interaction. The well dispersion of graphene and the enhanced interfacial interaction lead to a remarkable improvement in the electrical conductivity and mechanical properties. A percolation threshold as low as 0.12 vol.% of graphene has been achieved because of the formation of a three dimensional conductive network. Meanwhile, with the incorporation of as low as 0.5 wt% of graphene, the tensile strength of the nanocomposite has already displayed a two-fold increase compared with that of pure SBS.

Keywords Graphene · SBS · Interfacial interaction · Conductivity · Mechanical properties

H. Li · S. Wu · J. Wu (✉) · G. Huang (✉)
College of Polymer Science and Engineering, State Key Laboratory of Polymer Materials Engineering, Sichuan University, Chengdu 610065, People's Republic of China
e-mail: wujinrong@scu.edu.cn
e-mail: Guangsu-huang@hotmail.com

Introduction

As one of the most important thermoplastic elastomers, styrene-butadiene-styrene triblock copolymer (SBS) has attracted much attention in recent years due to the fact that it possesses advantages of both conventional rubbers and plastic polymers, which originate from its unique microphase separation [1]. To expand the application fields of SBS, it is a common practice to incorporate various fillers into SBS to improve the mechanical property and impart it with some functionalities, such as electrical conductivity, thermal conductivity, and permeability resistance [2–4]. For instance, to enhance the electrical conductivity of SBS, conductive carbon black is added with a high loading to achieve the percolation threshold. Nevertheless, too much carbon black impedes the microphase separation of SBS, thus strongly deteriorates the mechanical properties of the resulting composite [5]. The addition of carbon nanotubes (CNTs) can reduce the content of conductive filler required to achieve adequate conductivity, thus minimizes the influence on the microphase separation and the mechanical properties [3, 6–8]. Unfortunately, the dispersion of CNTs is difficult due to their insolubility in most solvents, moreover, the high cost of CNTs also limits their practical application.

Graphene, a novel 2D carbon nanomaterial with excellent electrical, thermal and mechanical properties [9–11], has provoked much research interest recently. Graphene can be produced by the chemical vapor deposition (CVD), mechanical cleavage, reduction of graphene oxide (GO) and so on. In the scalable chemical route, graphite is oxidized into GO which can be readily exfoliated in water and many other organic solvents such as *N, N*-dimethylformamide (DMF) and *N*–methyl pyrrolidone (NMP) [12, 13]. This provides a very convenient way for the implementation of solution-phase techniques toward the preparation of graphene-based polymers [14–18]. To date, however, only a few works have

investigated graphene-filled thermoplastic elastomers [19–21]. Liu et al. prepared SBS stabilized graphene from natural graphite under sonication, the electrical conductivity of the resulting SBS/graphene (SBS/GE) nanocomposites was up to 13 S/m [19]. However, sonication inevitably leads to degradation of polymers and is energy consuming, moreover, its large-scale preparation is limited. On the contrary, GO can be obtained in large quantity, but has poor compatibility with SBS. Thus, SBS was first hydroxylated and then mixed with chemical reduced graphene oxide to prepare graphene-based nanocomposites. Although the electrical conductivity of the resulting nanocomposites was improved, the mechanical property was deteriorated due to the destruction of phase separation derived from the interaction between chemical reduced graphene and polymer [21]. A similar result was reported by Peponi et al.[20] who prepared styrene-isoprene-styrene tri-block copolymer/graphene (SIS/GE) nanocomposites using solution blending method. The confinement to the phase separation of SIS, owing to the presence of the thermal reduced graphene in the nanocomposites, is probably adverse to the mechanical properties.

In this work, SBS/GE nanocomposites were prepared by a method of solution mixing and in situ reduction. It is shown that the graphene nanosheets are homogenuously dispersed and have strong interfacial interaction with the SBS matrix. Moreover, the microphase separation of SBS in the nanocomposites can be recovered after a thermal annealing process, albeit the variation of GE loading. As a result, both the electrical conductivity and the mechanical property of the nanocomposites are significantly improved. Thus, this method provides a simple way to obtain strong, stretchable and electrically conductive thermoplastic elastomers.

Experimental part

Materials

SBS with a polydispersity index (PDI) of 1.18 was purchased from Baling Petrochemical co., Ltd. (SBSYH792). The weight-averaged molecular weight (Mw) of SBS is 1.15×10^5 g·mol^{-1}. The weight fraction of PS blocks determined by ^{1}H NMR is 0.395. The flake graphite powder was purchased from Qingdao Ruisheng Graphite Co. Ltd, China with an average diameter of 1 μm. All other reagents were directly used without further purification.

Sample preparation

An appropriate amount of graphene oxide (GO), which was prepared by the Hummers′ method, was dispersed in NMP with ultrasonic treatment. Then 100 mL SBS/NMP solution (5 wt%) was added dropwise and stirred for another 6 h.

Reduction of the dispersed GO was carried out with hydrazine hydrate (1 mL for 20 mg GO) at 80 °C for 24 h. The polymer nanocomposite was precipitated by adding the NMP solution dropwise into a large volume of vigorously stirred methanol (10:1 with respect to the volume NMP used). The precipitated nanocomposite powder was isolated via filtration and dried under vacuum at 70 °C for 24 h to remove the residual solvent. The various SBS/GE nanocomposites were first dissolved in toluene to obtain a 5 wt% solution. The solvent was allowed to evaporate at room temperature. The film was then dried at 40 °C for 24 h to remove the excess solvent and annealed for 48 h at 120 °C. The samples were designated as G-SBS-n, in which n indicates the amount of graphene. For instance, G-SBS-05 represents SBS containing 0.5 wt% of graphene.

Ultracentrifugation and extraction of SBS/GE solution

Certain amount of SBS/GE nanocomposites was dissolved in toluene. Then, the suspension was centrifuged at 10,000 rpm for 60 min, and the supernatant solution was decanted. More successive centrifugation/redissolution cycles [22] were employed to separate the graphene from the physically absorbed polymer. The centrifugation and dissolution cycle was as follows: the obtained centrifugate was dissolved in the toluene again for 2 h and then separated by centrifugation again. The resulting solid material was washed extensively with methanol to remove any free SBS. The collected black solid was dried at 70 °C under vacuum for 24 h and designated as G -a- SBS.

Characterization

Raman spectroscopy

Raman spectra were recorded from 800 to 2,500 cm^{-1} on a LABRAM HR800 confocal micro-Raman spectrometer using a 532 nm ND: YAG laser.

X-ray photoelectron spectra

The X-ray photoelectron spectra (XPS) were performed with a Kratos XSAM800 instrument (Kratos Ltd, UK) using monochromatized Al Kα (1486.6 eV) X-radiation.

XRD and Optical microscopy

X-ray diffraction experiments were performed at room temperature with a X′ Pert Pro MPD (Philips) diffractometer (Cu Ka radiation, X-ray wavelength 1.5406 Å). Optical microscopy was done with a Leica DMIP polarizing light microscope.
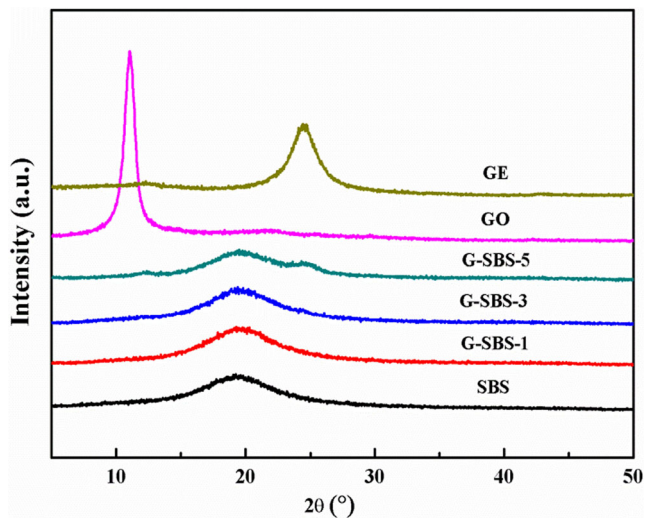
Fig. 1 XRD patterns of SBS, GO, GE and SBS/GE nanocomposites

Morphological characterization

Transmission electron microscopy (TEM) observations were performed on a TECNAI G^2 F20 apparatus with an acceleration voltage of 200 kV. Ultrathin sections of the nanocomposites were prepared at −100 °C using a Leica EM VC6/FC6 ultramicrotome with a diamond knife. These sections was collected and stained by osmium tetroxide (OsO$_4$) prior to the transmission electron microscopy (TEM) imaging.

Synchrotron small-angle X-ray scattering (SAXS) experiments were carried out under room temperature at BL16B1 beam-line in the Shanghai Synchrotron Radiation Facility (SSRF). The wavelength used was 0.124 nm. The film samples were directly used for SAXS measurments. The exposure time is 200 s for each measurement.

TGA

Thermal gravimetric analyses (TGA) were conducted at 10 °C/min from room temperature to 700 °C under a nitrogen flow using a TG 209 F1 analyzer (NETZSCH, Germany).
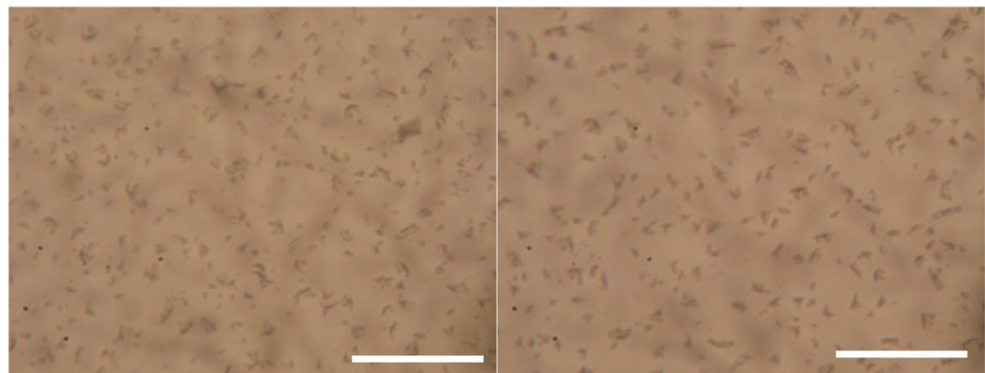
Properties characterization

Tensile tests were performed on dumbbell-shaped samples using a tensile testing machine, Instron 5567 at 23 °C with 50 % relative humidity. The extension rate was 50 mm/min and the load cell was 1000 N with a gauge length of 20 mm. The electrical conductivities higher than 10^{-6} S/m were measured with picoammeter (Keithley 6487) using a standard four-probe technique; the electrical conductivities below 10^{-6} S/m were measured using a ZC 36 high-resistance meter.

Results and discussion

Dispersion of GE in the SBS/GE nanocomposites

The irreversible agglomerates of graphene have become a major challenge for achieving homogeneous distribution within the polymer matrix. In this study, a simple and efficient method is applied to produce SBS/GE nanocomposites with the aid of π-π interaction between graphene and SBS matrix.

The dispersion state of graphene in the SBS matrix was firstly evaluated by XRD measurements. Figure 1 shows the X-ray diffraction patterns of pure SBS, GO, GE and SBS/GE nanocomposites. The diffraction pattern of GO shows a peak with a maximum at $2\theta=11°$ that corresponds to a $d_{spacing}$ of 8.03 Å. After reduction, the peak of GE becomes broad and shifts to a wider angle up to 24.6° corresponding to an interlayer spacing of 3.61 Å, which is presumably induced by the removal of the most of oxygen functional groups. Pure SBS shows a diffuse-like peak at $2\theta=19°$, indicating the amorphous nature of SBS. When the content of GE is no more than 3 wt%, the SBS/GE nanocomposites have only one broad peak corresponding to the diffraction of SBS matrix. Except this peak, no characteristic peak of graphene in the nanocomposites is detected, thus it can be inferred that graphene nanosheets are well exfoliated in the SBS matrix. However, when the graphene content is up to 5 wt%, a slight shoulder corresponding approximately to the interlayer spacing of GE

Fig. 2 Optical micrographs of the SBS/GE nanocomposites containing 3 wt% of graphene (left) and 5 wt% of grapheme (right). The scale bar in the figure is 50 μm

Fig. 3 (a) Raman spectra of GO, GE and G-*a*-SBS; (b)~(d) The C 1 s peak in the XPS spectra of GO, GE and G-*a*-SBS
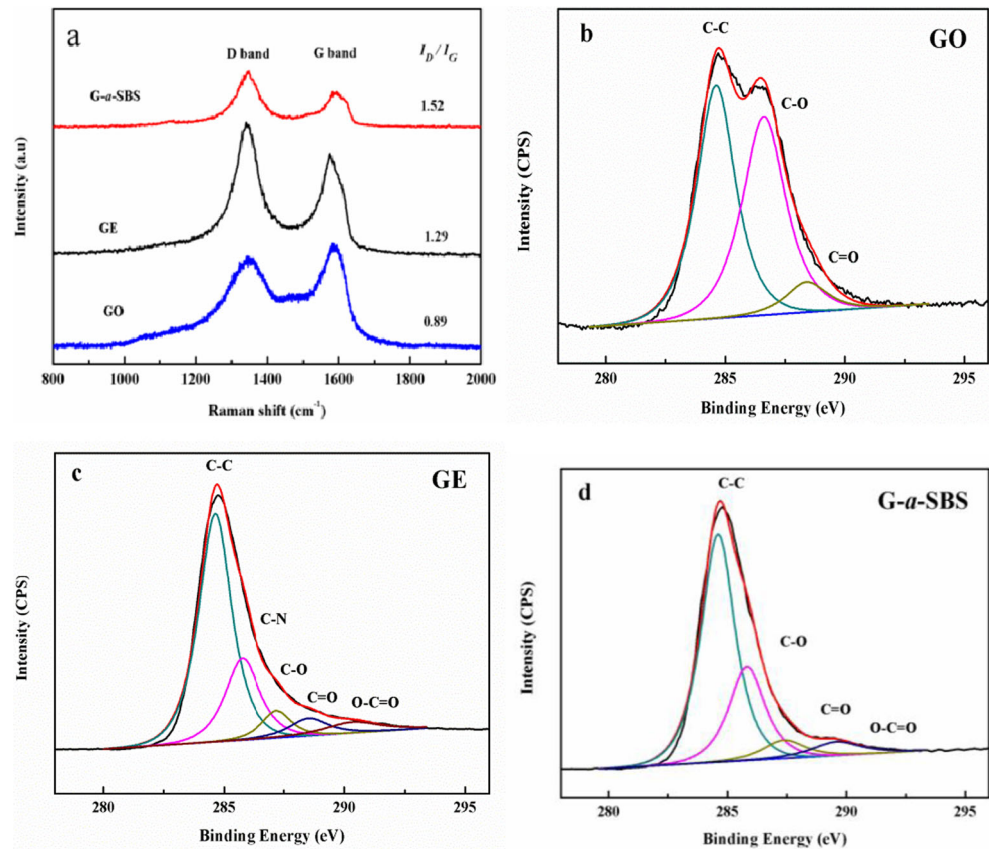
emerges, suggesting the presence of layer-by-layer restacking of graphene [23].

Optical microscopy was further employed to analyze the dispersion of graphene in the SBS matrix. Figure 2 shows the optical micrographs of the SBS/GE nanocomposites with 3 wt% and 5wt % loading of GE, respectively. It is clear that the graphene nanosheets are finely dispersed in the SBS matrix without any obvious aggregation. This result,

combined with XRD results, indicates that GE is well exfoliated and dispersed in the SBS matrix.

Reduction of GO in the nanocomposites

Raman spectroscopy has historically played an important role in the structural characterization of graphitic materials [24–26]. It can provide useful information on the structure
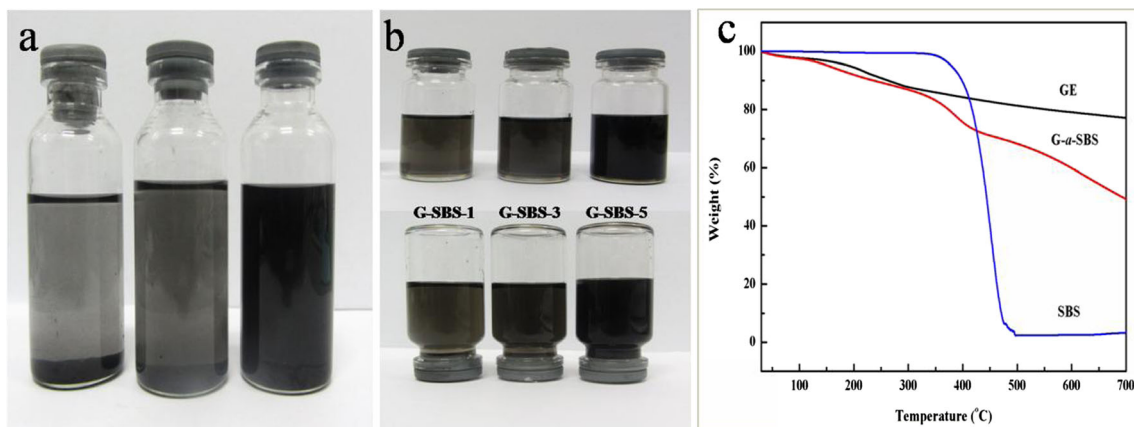

Fig. 4 **a** digital photographs of GE suspension (left), simple mixture of GE and SBS (middle) and SBS/GE nanocomposite suspension (right); **b** digital photos of toluene supernatants of the SBS/GE nanocomposites

obtained by centrifugated at 10,000 rpm for 60 min (up) and after being aged for 1 month showing no precipitate (down); **c** TGA curves of pure SBS, GE and G-*a*-SBS samples
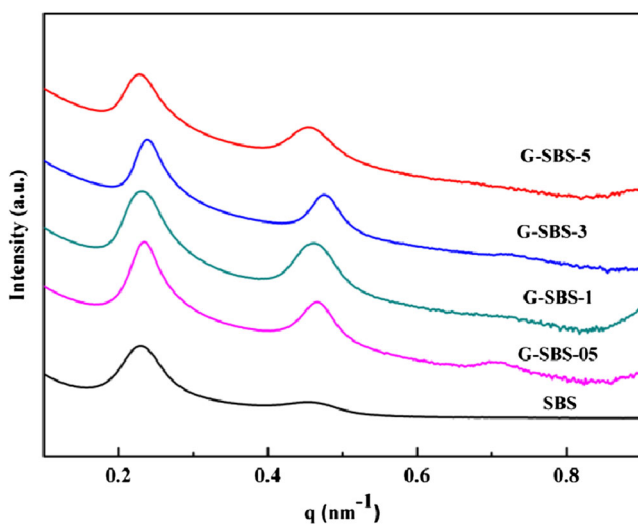
Fig. 5 SAXS profiles for pure SBS and composites with different loading

defects (D band) and in-plane vibration of sp^2 carbon atoms (G band). The Raman spectra of GO, GE and G-a-SBS are plotted in Fig. 3a. As shown in Fig.3a, GO exhibits a G band and a D band at 1,586 cm^{-1} and 1,346 cm^{-1}, respectively. After reduction, the G band of GE shows a red shift to 1,576 cm^{-1} which is attributed to the restoration of sp^2 hybridized carbon atoms as new graphitic domains [27, 28]. In case of G -a- SBS, a shift of the G band to a high frequency is observed, suggesting that the number of stacked graphene layers is decreased at the presence of SBS compared with that of GE and GO [29, 30]. The intensity ratio of D band to G band (I_D/I_G) is further employed to evaluate the transformation from graphene oxide to graphene. The value of I_D/I_G is increased from 0.89 for GO to 1.52 for G-a-SBS and 1.29 for GE, which is attributed to the formation some new and small sp^2 domains [24, 27, 31].

To further confirm the reduction of GO, X-ray photoelectron spectroscopy (XPS) was measured for GO, GE and G-a-

SBS (Fig. 3b~d). The C1s XPS spectrum of GO (Fig. 3b) clearly indicates a considerable degree of oxidation with two main oxidized carbon peaks: the C in C–O bonds (including hydroxyl and epoxy groups, 286.6 eV) and the C in C = O bonds (carbonyl group, 288.4 eV). Although the C1s XPS spectra of GE and G-a-SBS (Fig. 3c) also exhibit the same oxygen functionalities that have been assigned for GO, the peak intensities of these components in the reduced samples are significantly suppressed, indicating considerable deoxygenation by the reduction process. Moreover, the C/O atomic ratio increases from 3.3 for GO to 11.8 for G-a-SBS and 12.3 for GE. These results, combined with Raman measurement, indicate a successful reduction of GO to graphene.

Interfacial interaction between SBS and graphene

The interfacial interaction between SBS and GE was examined through a dissolution experiment in the organic solvents. SBS matrix was soluble in some organic solvents, such as toluene, in which GE is insoluble. Figure 4a shows the photographs of the toluene solutions of GE, SBS/GE nanocomposite and the simple mixture of SBS and GE (the concentration of GE is about 0.2 mg/ml in all the samples). It can be seen that GE precipitates at the bottom of vial and the dispersion of GE can not be improved by simply mixing with SBS. In contrast, the SBS/GE nanocomposite with 3 wt % of graphene is soluble in toluene, exhibiting a unique black without precipitates. This can give us a direct impression of the existence of interaction between CRG and SBS, which stabilizes the graphene nanosheets in toluene. Ultracentrifugation experiment was also used to evaluate the interfacial interaction between filler and polymer [32]. Figure 4b shows the photographs of supernatants decanted from the solution of SBS/GE nanocomposites (the concentration of solutions is 5 wt %) after being centrifuged at 10,000 rpm for 60 min. Generally speaking, phase separation of graphene from the

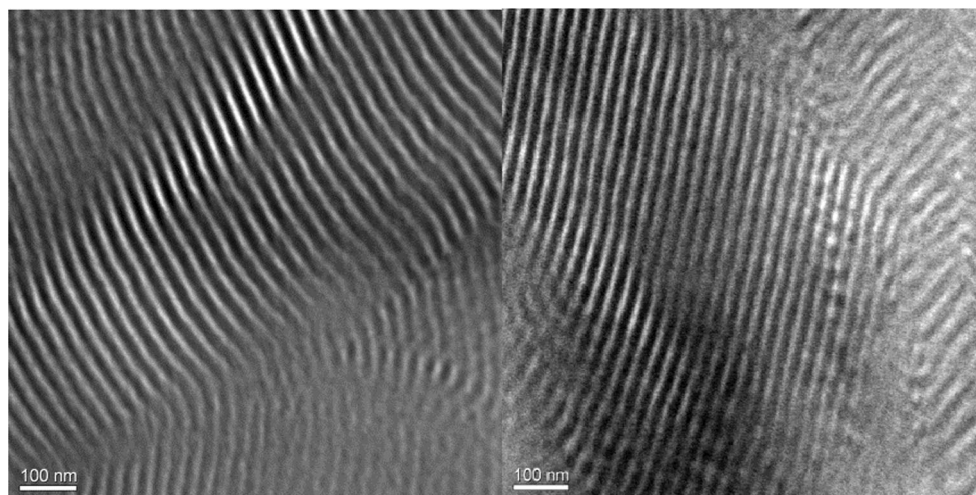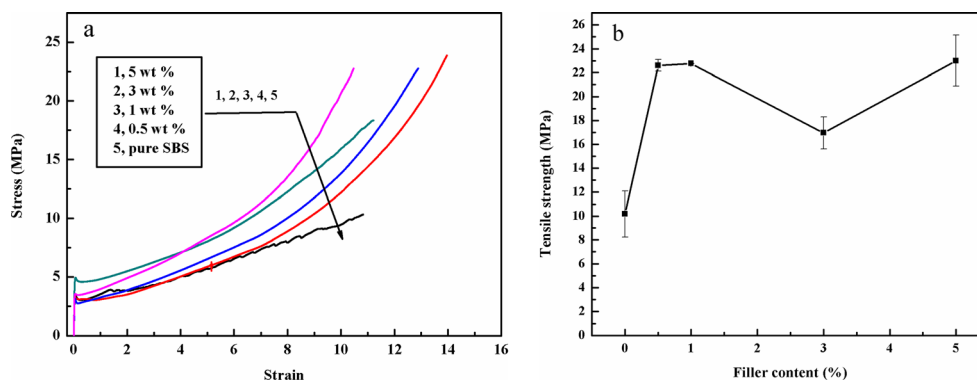**Fig. 6** TEM images of pure SBS (left) and SBS/GE nanocomposite with 3 wt % graphene loading (right)

Fig. 7 a Stress–strain curves of pure SBS and various SBS/GE nanocomposites; **b** Tensile strength of various SBS/GE nanocomposites. The error bars indicate standard deviations of the five parallel measurements

solutions of SBS/GE nanocomposites under strong centrifugal force could occur, due to the density difference between GE and toluene and the poor solubility of GE in toluene. However, the black supernatants can be observed even after an extremely strong ultracentrifugation and remain stable even after 1 month, indicating the occurrence of strong interfacial interaction between GE and SBS during the solution mixing and in situ reduction process. The strong interfacial interaction leads to the absorption of SBS molecules onto the surfaces of GE nanosheets. TGA measurement was used to determine the content of wrapped SBS on the GE nanosheets. The TGA curves are shown in Fig. 4c. GE and G-a-SBS exhibit the oxygen functionalities after reduction which is seen from the XPS. It is reported that graphene oxide was reduced in the organic media such as DMF, NMP et al. using hydrazine hydrate which is not supposed to reduce the carboxylic groups [33]. Therefore, the weight loss of GE and G-a-SBS between 200 °C and 300 °C can be attributed to loss of carboxylic groups. While the major weight loss of G-a-SBS occur in the temperature range of 400–500 °C, corresponding to the decomposition of SBS. Considering that GE and pure SBS lost

22.9 wt% and 96.8 wt% of its original weight, the content of wrapped SBS in G-a-SBS sample was thus estimated to be about 60 %.

It has been demonstrated that graphene, as a two-dimensional sheet composed of sp^2 carbon atoms, can strongly interact with aromatic structures via π-stacking [34], which leads to the strong interfacial inetraction between GE and SBS. Therefore, SBS can be adsorbed onto the exfoliated graphene nanosheets and prevent them from restacking [19]. In other words, graphene could be well dispersed in the SBS matrix to produce SBS/GE nanocomposites.

Effect of graphene on the phase structure of SBS

As a block copolymer, SBS undergoes microphase separation into self-assembled ordered morphologies, which is of critical importance for its mechanical properties [35, 36] . Therefore, it is necessary to investigare the microphase separation of pure SBS and SBS/GE nanocomposites with different contents of graphene.

Fig. 8 Electrical conductivity of SBS/GE nanocomposites with different loading
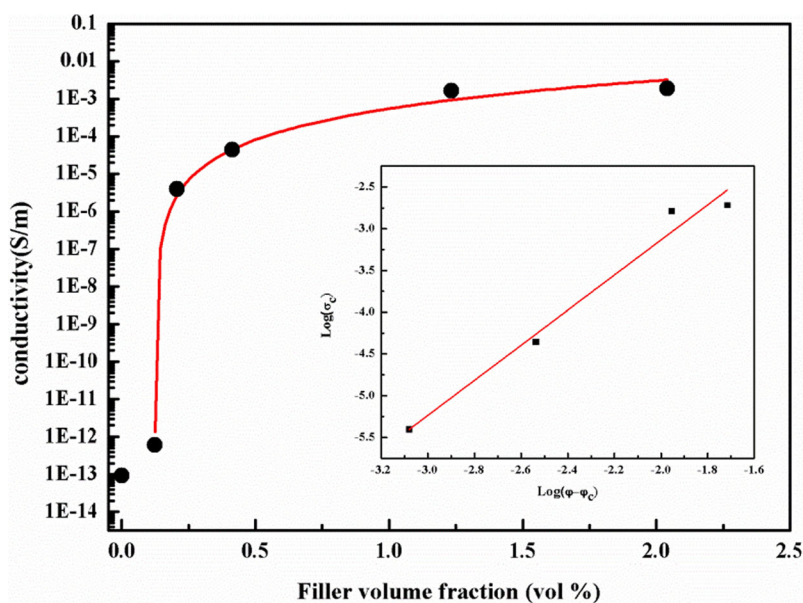
SAXS measurements were performed to investigate the microphase separation of pure SBS and SBS/GE nanocomposites which are annealed for 48 h at 120 °C. Figure 5 shows the SAXS profiles in which the X-ray intensity is plotted as a function of the scattering vector q. A q/q* ratio of 1:2:3 can be observed for the higher order scattering peaks to the primary peak of pure SBS, indicating existence of the typical lamellae microstructure. Similar with the pure SBS, the multiple scattering peaks of SBS/GE nanocomposites have almost the same peak position ratios, which suggests that the well-dispersed graphene does not change the morphology of microphase-separated SBS and that the SBS matrix maintains the lamellae structure in the nanocomposites.

Figure 6 shows the TEM images for pure SBS and its nanocomposite with 3 wt % graphene. The pure SBS has the lamellae structure. However, a highly ordered phase structure with the same morphology is still formed in the nanocomposite. Due to the slight difference of electron density between graphene and the SBS matrix, graphene was not observed in the field after staining with OsO_4. The TEM results are consistent with those observed from SAXS. In contrast, montmorillonite, with the similar layered structure, has been found to weaken or disturbthe microphase separation of block copolymer [37, 38]. The changes in the microphase separation could lead to a decrease of mechanical properties [38].

Mechanical properties

Figure 7a illustrates the representative stress–strain curves of SBS/GE nanocomposites with various loadings of GE. Figure 7b plots the tensile strength of SBS/GE nanocomposites as a functon of the graphene loading. It can be clearly seen that the tensile strength of SBS/GE nanocomposites at various loading are higher than that of pure SBS. More specifically, the tensile strength of SBS/GE nanocomposite with 0.5 wt% graphene is 23.8 MPa, more than two folds higher than that of pure SBS (10.5 MPa). The mechanical properties of SBS/GE nanocomposites depend on three factors, including the phase structure of SBS, the dispersion of graphene as well as the interfacial interaction between graphene and SBS. As mentioned above, the morphology of SBS remains unchanged upon addition of graphene. Therefore, the enhancement of mechanical properties can be attributed to the homogeneous dispersion of graphene and the strong interfacial interaction between GE and the SBS [32].

Electrical conductivity

The volume conductivity is plotted in Fig. 8 as a function of the graphene loading for the SBS/GE nanocomposites. As can be seen, the electrical conductivity of SBS/GE nanocomposites increases with increasing graphene loading. A sudden increase in the conductivity (i.e. the percolation phenomenon)

was observed as the mass fraction of graphene varies from 0.1 vol% to 0.2 vol%, indicating the formation of a preliminary conductive network. When the content of grahene is as low as 1.2 vol %, the electrical conductivity of the nanocomposite has attained a value of 1.64×10^{-2} S/m. Thereafter, the electrical conductivity of the nanocomposites stays on the same orders of magnitude with the further addition of graphene.

The conductivity of the nanocomposites can be fitted with a modified percolation theory, $\sigma = \sigma_0(\varphi - \varphi_c)^t$, where σ is the conductivity of the nanocomposite, φ is the volume fraction of the filler, φ_c is the volume percolation concentration, and t is the critical exponent which is related to the dimensionality of conductive network. The calculated value of φ_c is 0.12 vol%. This extremely low percolation concentration is consistent with those reported in previous works [19, 21] and can be attributed to the good exfoliation and dispersion of graphene. In addition, the calculated value of t is approximately 2.10, implying the presence of a three-dimensional network.

Conclusion

SBS/GE nanocomposites were successfully prepared by solution mixing and in situ reduction. The enhanced interfacial interaction between graphene and SBS resulting from the π-π intercation makes graphene difficult to re-aggregation and improves the dispersion of graphene in the SBS matrix. The dispersed graphene form an electrical conductive network at a relative low graphene loading (percolation threshold, 0.12 vol %). Moreover, the obtained SBS/GE nanocomposites exhibit significantly enhanced mechanical properties.

References

1. Adhikari R, Michler GH (2004) Influence of molecular architecture on morphology and micromechanical behavior of styrene/butadiene block copolymer systems. Prog Polym Sci 29(9):949–986
2. Lu L, Zhou Z, Zhang Y, Wang S, Zhang Y (2007) Reinforcement of styrene–butadiene–styrene tri-block copolymer by multi-walled carbon nanotubes via melt mixing. Carbon 45(13):2621–2627
3. Inukai S, K-i N, Noguchi T, Ueki H, Magario A, Yamada E, Inagaki S, Endo M (2011) Preparation and properties of multiwall carbon nanotubes/polystyrene-block-polybutadiene-block-polystyrene composites. Ind Eng Chem Res 50(13):8016–8022
4. Costa P, Silva J, Sencadas V, Simoes R, Viana JC, Lanceros-Méndez S (2012) Mechanical, electrical and electro-mechanical properties of thermoplastic elastomer styrene–butadiene–styrene/multiwall carbon nanotubes composites. J Mater Sci 48(3):1172–1179
5. Leyva ME, Barra GMO, Moreira ACF, Soares BG, Khastgir D (2003) Electric, dielectric, and dynamic mechanical behavior of

carbon black/styrene-butadiene-styrene composites. J Polym Sci Pol Phys 41:2983–2997

6. Li Y, Shimizu H (2009) Toward a stretchable, elastic, and electrically conductive nanocomposite: morphology and properties of poly[styrene-b- (ethylene-co -butylene)- b-styrene]/multiwalled carbon nanotube composites fabricated by high-shear processing. Macromolecules 42:2587–2593

7. Shafee EE, Gamal ME, Isa M (2011) Electrical properties of multi walled carbon nanotubes/poly(vinylidene fluoride/trifluoroethylene) nanocomposites. J Polym Res 19:9805–9812

8. Gupta TK, Singh BP, Teotia S, Katyal V, Dhakate SR, Mathur RB (2013) Designing of multiwalled carbon nanotubes reinforced polyurethane composites as electromagnetic interference shielding materials. J Polym Res 20(6):169

9. Du X, Skachko I, Barker A, Andrei EY (2008) Approaching ballistic transport in suspended graphene. Nature Nanotechnology 3(8): 491–495

10. Balandin AA, Ghosh S, Bao W, Calizo I, Teweldebrhan D, Miao F, Lau CN (2008) superior thermal conductivity of single-layer graphene. Nano Lett 8:902–907

11. Lee C, Wei X, Kysar JW, Hone J (2008) Measurement of the elastic properties and intrinsic strength of monolayer graphene. Science 321(5887):385–388

12. Paredes JI, Villar-Rodil S, Martínez-Alonso A, Tascón JMD (2008) Graphene oxide dispersions in organic solvents. Langmuir 24: 10560–10564

13. Dreyer DR, Park S, Bielawski CW, Ruoff RS, Botany BJO (2010) The chemistry of graphene oxide. Chem Soc Rev 39:228–240

14. Stankovich S, Dikin DA, Geoffrey HB, Dommett KM, Kohlhaas EJ, Zimney EA, Stach RD, Piner NST, Ruoff RS (2006) Graphene-based composite materials. Nature 442:282–286

15. Kim H, Miura Y, Macosko CW (2010) Graphene/polyurethane nanocomposites for improved gas barrier and electrical conductivity. Chem Mater 22(11):3441–3450

16. Yoonessi M, Gaier JR (2010) Highly conductive multifunctional graphene polycarbonate nanocomposites. ACS Nano 4:7211–7220

17. Li H, Wu S, Wu J, Huang G (2013) A facile approach to the fabrication of graphene-based nanocomposites by latex mixing and in situ reduction. Colloid Polym Sci 291(10):2279–2287

18. Wu J, Huang G, Li H, Wu S, Liu Y, Zheng J (2013) Enhanced mechanical and gas barrier properties of rubber nanocomposites with surface functionalized graphene oxide at low content. Polymer 54(7): 1930–1937

19. Liu Y, Xie X, Ye X (2011) High-concentration organic solutions of poly(styrene-co-butadiene-co-styrene)-modified graphene sheets exfoliated from graphite. Carbon 49(11):3529–3537

20. Peponi L, Tercjak A, Verdejo R, Lopez-Manchado MA, Mondragon I, Kenny JM (2009) Confinement of functionalized graphene sheets by triblock copolymers. J Phys Chem C 113:17973–17978

21. Xiong Y, Xie Y, Zhang F, Ou E, Jiang Z, Ke L, Hu D, Xu W (2012) Reduced graphene oxide/hydroxylated styrene–butadiene–styrene tri-block copolymer electroconductive nanocomposites: Preparation and properties. Materials Science and Engineering: B 177(14): 1163–1169

22. Liu K, Chen L, Chen Y, Wu J, Zhang W, Chen F, Fu Q (2011) Preparation of polyester/reduced graphene oxide composites via in situ melt polycondensation and simultaneous thermo-reduction of graphene oxide. J Mater Chem 21(24):8612

23. Potts JR, Om S, Ling D, Ruoff RS (2012) Processing–morphology–property relationships and composite theory analysis of reduced graphene oxide/natural rubber nanocomposites. Macromolecules 45:6045–6055

24. Ferrari AC, Robertson J (2000) Interpretation of Raman spectra of disordered and amorphous carbon. Phys Rev B 61:14095–14107

25. Malard LM, Pimenta MA, Dresselhaus G, Dresselhaus MS (2009) Raman spectroscopy in graphene. Physics Reports 473(5–6):51–87

26. Pimenta MA, Dresselhaus G, Dresselhaus MS, Cancado LG, Jorio A, Saito R (2007) Studying disorder in graphite-based systems by Raman spectroscopy. Phys Chem Chem Phys 9(11):1276

27. Dang TT, Pham VH, Hur SH, Kim EJ, Kong BS, Chung JS (2012) Superior dispersion of highly reduced graphene oxide in N, N-dimethylformamide. J Colloid Interface Sci 376(1):91–96

28. Pham VH, Dang TT, Cuong TV, Hur SH, Kong B-S, Kim EJ, Chung JS (2012) Synthesis of highly concentrated suspension of chemically converted graphene in organic solvents: effect of temperature on the extent of reduction and dispersibility. Korean J Chem Eng 29(5): 680–685

29. Shen J, Hu Y, Shi M, Lu X, Qin C, Li C, Ye M (2009) Fast and facile preparation of graphene oxide and reduced graphene oxide nanoplatelets. Chem Mater 21(15):3514–3520

30. Rao CNR, Biswas K, Subrahmanyam KS, Govindaraj A (2009) Graphene, the new nanocarbon. J Mater Chem 19(17):2457

31. Stankovich S, Dikin DA, Piner RD, Kohlhaas KA, Kleinhammes A, Jia Y, Wu Y, Nguyen ST, Ruoff RS (2007) Synthesis of graphene-based nanosheets via chemical reduction of exfoliated graphite oxide. Carbon 45(7):1558–1565

32. Shen B, Zhai WT, Tao MM, Lu DD, Zheng W (2013) Enhanced interfacial interaction between polycarbonate and thermally reduced graphene induced by melt blending. Compos Sci Technol 86: 109–116

33. Villar-Rodil S, Paredes JI, Martínez-Alonso A, Tascón JMD (2009) Preparation of graphene dispersions and graphene-polymer composites in organic media. J Mater Chem 19(22):3591–3593

34. Chen RJ, Zhang Y, Wang D, Dai H (2001) Noncovalent sidewall functionalization of single-walled carbon nanotubes for protein immobilization. J Am Chem Soc 123:3838–3839

35. Orimo Y, Hotta A (2011) Stress–strain behavior, elastic recovery, fracture points, and time–temperature superposition of an oot-possessing triblock copolymer. Macromolecules 44(13):5310–5317

36. Zhao Y, Ning N, Hu X, Li Y, Chen F, Fu Q (2012) Processing temperature dependent mechanical response of a thermoplastic elastomer with low hard segment. Polymer 53(19):4310–4317

37. Zhang Z, Zhang L, Li Y, Xu H (2006) Styrene-butadiene-styrene/montmorillonite nanocomposites synthesized by anionic polymerization. J Appl Polym Sci 99(5):2273–2278

38. Lee CH, Kim HB, Lim ST, Kim HS, Kwon YK, Choi HJ (2006) Ordering behavior of layered silicate nanocomposites with a cylindrical triblock copolymer. Macromol Chem Phys 207(4):444–455